

A Mach-Zehnder Interferometer on a Photonic Integrated Circuit

John D. Garrett, *Member, IEEE*

I. INTRODUCTION

TRADITIONAL optical circuits require large optical tables. However, we can leverage CMOS technology to build optical circuits on silicon wafers, called *photonic integrated circuits* (PICs). PICs are now being used in a variety of different applications, but most commonly in high-speed data transmission.

A. Silicon-on-insulator photonic integrated circuits

Silicon-on-insulator (SOI) wafers are commonly used in high-performance electronics as a result of the lower capacitance and leakage current offered by the buried oxide layer. However, they also offer an excellent platform for optical waveguides. A common SOI wafer composition for multi-project wafers is 220 nm thick silicon layer on top of a $\sim 2 - 3 \mu\text{m}$ silicon dioxide layer (i.e., the *buried oxide layer* or *BOX*), which is all on top of the bulk silicon substrate.

To create an optical waveguide, we need a channel made from a material with a high refractive index surrounded by a material with a low refractive index. For SOI-based PICs, the waveguides are made in the top silicon layer ($n_{\text{Si}} = \sqrt{\epsilon_r, \text{Si}} \approx 3.47$ where ϵ_r is the relative permittivity), which sits on top of the buried oxide layer ($n_{\text{SiO}_2} = \sqrt{\epsilon_r, \text{SiO}_2} \approx 1.44$). After etching the waveguide, a top cladding layer is typically deposited, providing a silicon channel completely surrounded by silicon dioxide. The approximate dielectric properties of silicon (Si) and silicon dioxide (SiO₂) are summarized in Table I. Note that SiO₂ has a much weaker dependence on temperature and wavelength.

II. STRIP WAVEGUIDE MODELLING

For this first design, I kept the design parameters very simple in order to achieve at least one working design. I chose to use the TE polarization with a waveguide height of 220 nm and a width of 500 nm. I simulated these waveguide dimensions using a finite-difference eigenmode solver (Ansys

e-mail: john.daniel.garrett@gmail.com, edX username: JG_2409_D6M4, GitHub username: [garrettj403](#)

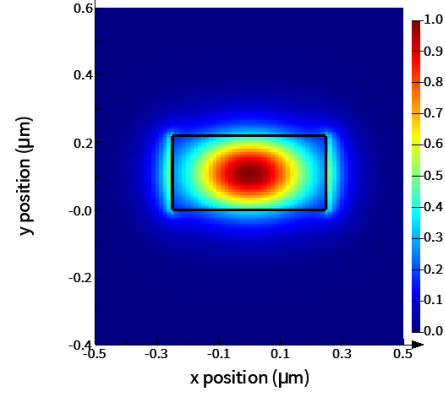


Fig. 1. The electric field intensity at $\lambda = 1550 \text{ nm}$. Simulated using a finite-difference eigenmode solver (Ansys Lumerical MODE). Note that this plot is cropped to fit the waveguide. The total simulation area was $2.5 \mu\text{m} \times 1.7 \mu\text{m}$.

Lumerical MODE). The simulated electric field intensity at $\lambda = 1550 \text{ nm}$ is plotted in Fig. 1. For the TE mode at $\lambda = 1550 \text{ nm}$, the simulated effective index is $n_{\text{eff}} = 2.4446$, the group index is $n_g = 4.1967$, and the TE polarization fraction is 0.98, meaning that it is almost entirely TE. The simulated loss is 0.0004 dB/cm, but this simulation does not include the roughness of the sidewalls, which is the dominant source of loss in real waveguides.

The simulated effective index and group index are plotted in Fig. 2 as a function of wavelength. The effective index data was fitted with a second-order polynomial model to produce the following *compact model*:

$$n_{\text{eff}} \approx 2.4446 - 1.130 \cdot (\lambda - 1.55) - 0.04 \cdot (\lambda - 1.55)^2 \quad (1)$$

where the wavelength λ is in units of μm . The compact model has excellent agreement with n_{eff} , as seen in Fig. 2. The group index is related to the effective index by:

$$n_g = n_{\text{eff}} - \lambda \frac{dn_{\text{eff}}}{d\lambda} \quad (2)$$

From the effective index and phase index, we can calculate the phase and group velocities by:

$$v_p(\lambda) = \frac{c}{n_{\text{eff}}(\lambda)} \quad (3)$$

$$v_g(\lambda) = \frac{c}{n_g(\lambda)} \quad (4)$$

where c is the speed of light in a vacuum. Note that silicon waveguides are dispersive, meaning that different frequencies travel at different velocities. In a dielectric waveguide, note

TABLE I
FIRST-ORDER WAVELENGTH AND TEMPERATURE DEPENDENCE OF
SILICON AND SILICON OXIDE.

Property	Si	SiO ₂
n	3.47	1.44
ϵ_r	12.0	2.07
$dn/d\lambda$	$-7.6 \times 10^{-5} \text{ nm}^{-1}$	$-1.2 \times 10^{-5} \text{ nm}^{-1}$
dn/dT	$1.87 \times 10^{-4} \text{ K}^{-1}$	$8.5 \times 10^{-6} \text{ K}^{-1}$

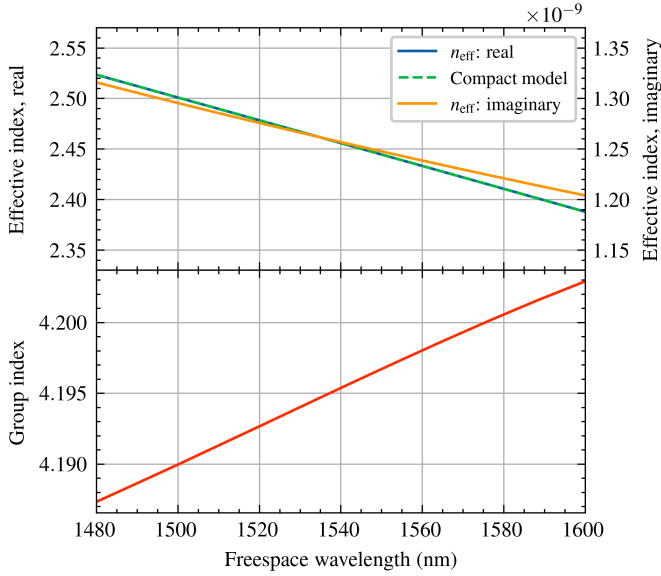


Fig. 2. Simulated properties of the TE mode for a $500\text{ nm} \times 220\text{ nm}$ waveguide. These results were simulated using a finite-difference eigenmode solver (Ansys Lumerial MODE).

that the group velocity is slower than the phase velocity, meaning that the phase fronts appear to travel faster than the pulse envelope.

III. PIC DESIGN

A. Imbalanced Mach-Zehdner Interferometer

Mach-Zehdner interferometers (MZI) are common optical devices used in PICs to create switches and filters. They are constructed using simple waveguides and Y-branch splitters, as well as fiber grating couplers for the input and output signals.

The transfer function of a lossless imbalanced MZI is:

$$\frac{I_o}{I_i} = \frac{1}{2} [1 + \cos(\beta \Delta\ell)] \quad (5)$$

where I_i and I_o are the input and output intensity, respectively; β is the propagation constant and $\Delta\ell$ is the length mismatch between the two branches of the MZI.

The goal of this design is to extract the group index from the MZI transmission spectra. The free spectral range (FSR) of an imbalanced MZI is:

$$\text{FSR} \approx \frac{\lambda^2}{\Delta\ell n_g} \quad [\text{m}] \quad (6)$$

where $\Delta\ell$ is the length mismatch between the two legs of the MZI, λ is the free-space wavelength, and n_g is the ground index. Therefore, by measuring the distance between the minima in the transmission spectra, we can extract the group index.

A target of 10 minima will give us enough samples within the C-band measurement window to see the shape of the group index. This corresponds to a length mismatch of:

$$\Delta\ell \approx \frac{\lambda^2}{\text{FSR} \cdot n_g} \quad [\text{m}] \quad (7)$$

TABLE II
SUMMARY OF MZI VARIATIONS.

Num. of minima	$\Delta\ell$ (μm)	FSR (nm)
10	60	10.0
20	120	5.0
30	180	3.3

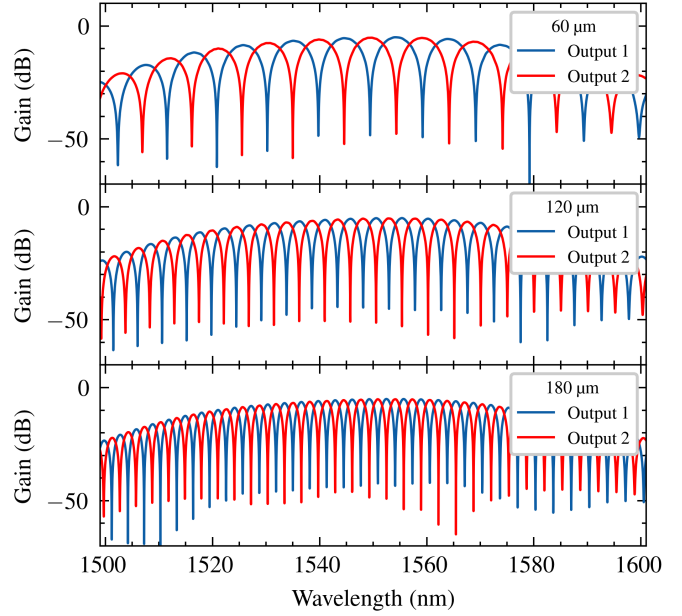


Fig. 3. Simulated gain of the imbalanced MZI with a length mismatch of $60\text{ }\mu\text{m}$, $120\text{ }\mu\text{m}$ and $180\text{ }\mu\text{m}$.

With a bandwidth of 100 nm , I want an FSR of $\sim 10\text{ nm}$ for 10 minima within the measurement window. Assuming $n_g \approx 4$, this gives a length mismatch of $\Delta\ell \approx 60\text{ }\mu\text{m}$. I can also create variants with 20 and 30 minima. These require length mismatches of $\Delta\ell \approx 120\text{ }\mu\text{m}$ and $\Delta\ell \approx 180\text{ }\mu\text{m}$, respectively. These design variants are summarized in Table II.

These length mismatch values were validated using Ansys Lumerial INTERCONNECT, along with the SiEPIC E-Beam PDK. The gain of the imbalanced MZI with $\Delta\ell \approx 60\text{ }\mu\text{m}$ is shown in Fig. 3. We can see 10 minima, as intended. The FSR at approximately 1556 nm is 9.2 nm . Rearranging Eq. 6, this is equivalent to a group index of:

$$n_g \approx \frac{\lambda^2}{\Delta\ell \cdot \text{FSR}} = 4.35 \quad (8)$$

IV. FABRICATION AND TESTING

The PICs presented in this report were fabricated and tested through the [openEBL](#) service offered through the Silicon Electronics-Photonics Integrated Circuits¹ (SiEPIC) program [1], [2]. For the February 2026 fabrication run, the PICs will be fabricated by Applied Nanotools, Inc. in Edmonton, Alberta, Canada.

The process begins with a 200 mm SOI wafer (Soitec UNIBOND). This wafer features a 220 nm silicon layer on top of a $3.017\text{ }\mu\text{m}$ buried oxide layer. A negative resist is

¹<https://siepic.ca/>

then applied (Hydrogen Silsesquioxane, HSQ²). The resist is patterned using electron-beam lithography (e-beam, JEOL JBX-6300FS). The mask data preparation for the e-beam tool is performed by the “Beamer” software package. Everything not covered by the negative photoresist is then fully etched using an inductively coupled plasma (ICP) process. This results in a sidewall angle of $\sim 82^\circ$ on the photonic circuit elements. The minimum allowed isolated feature size is 60 nm. The shot pitch is 6 nm, meaning that all features will be snapped to a 6 nm grid. Therefore, all optical structures should use dimensions that are an integer number of 6 nm to avoid quantization errors.

The final step is the deposition of a 2–3 μm oxide cladding layer using plasma-enhanced chemical vapour deposition (PECVD).

Each designer is allowed an area of $605 \mu\text{m} \times 410 \mu\text{m}$. This is enough room to fit approximately 5–10 simple photonic circuits, such as Mach-Zehdner and Michelson interferometers.

The openEBL program offers automated optical measurements in the C-band, between approximately 1500 and 1600 nm; therefore, any spectral features that I intend to measure must fall within this range. The measurements will be conducted at 25°C.

To work with the automated testing setup, the grating couplers (GCs) must follow a specific sequence. A maximum of four grating couplers is allowed. They must be arranged in a column with a spacing of 127 μm . They must all be rotated such that the waveguide exits from the right-hand side. Counting from the top GC, the second GC is the input and all of the other GCs are outputs. Note that we don’t need to use all four GCs, e.g., we could choose to only use 2–4, meaning that the input is actually the top GC.

V. MEASUREMENT RESULTS & ANALYSIS

Work in progress.

VI. CONCLUSION

Work in progress.

REFERENCES

- [1] L. Chrostowski, Z. Lu, J. Flueckiger, X. Wang, J. Klein, A. Liu, J. Jhoja, and J. Pond, "Design and simulation of silicon photonic schematics and layouts," in *Proc. SPIE 9891, Silicon Photonics and Photonic Integrated Circuits V*, 989114, May 2016.
- [2] L. Chrostowski, H. Shoman, M. Hammond, H. Yun, J. Jhoja, E. Luan, S. Lin, A. Mistry, D. Witt, N. A. F. Jaeger, S. Shekhar, H. Jayatilleka, P. Jean, S. B.-de Villers, J. Cauchon, W. Shi, C. Horvath, J. N. Westwood-Bachman, K. Setzer, M. Aktary, N. Shane Patrick, R. Bojko, A. Khavasi, X. Wang, T. Ferreira de Lima, A. N. Tait, P. R. Prucnal, D. E. Hagan, D. Stevanovic, and A. P. Knights, "Silicon Photonic Circuit Design Using Rapid Prototyping Foundry Process Design Kits," *IEEE Journal of Selected Topics in Quantum Electronics*, Vol. 25, No. 5, Sep. 2019.
- [3] E. D. Palik, *Handbook of Optical Constants of Solids*. New York, NY, USA: Academic Press, 1985.

²<https://ebeam.mff.uw.edu/ebeamweb/process/process/hsq.html>